Cell Reports

PRDM12 Is Required for Initiation of the Nociceptive Neuron Lineage during Neurogenesis

Graphical Abstract

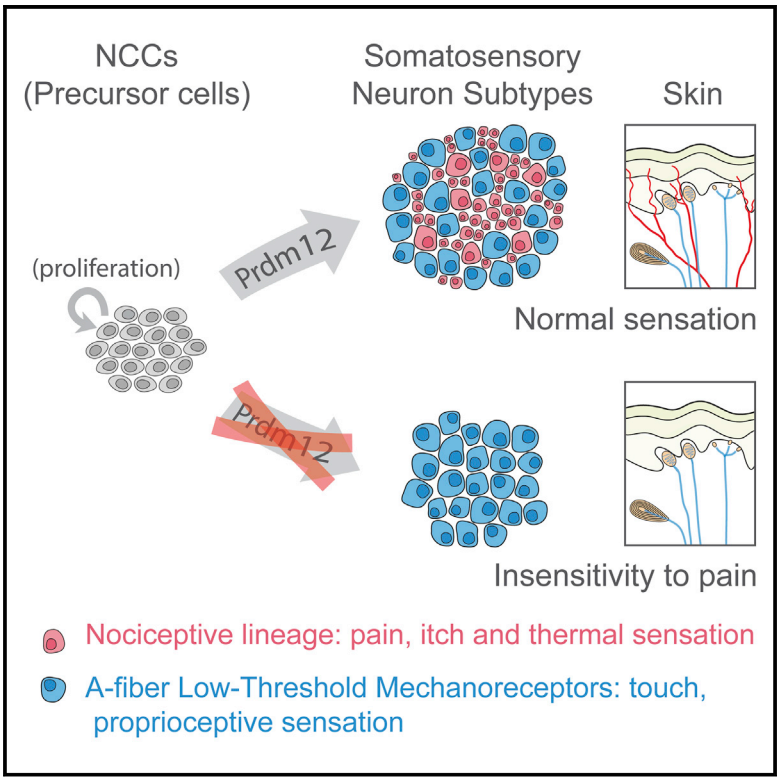

Authors

Luca Bartesaghi, Yiqiao Wang, Paula Fontanet, ..., Francois Lallemend, Saida Hadjab, Roman Chrast

Correspondence

francois.lallemend@ki.se (F.L.), saida.hadjab@ki.se (S.H.), roman.chrast@ki.se (R.C.)

In Brief

The sensation of pain, temperature, and itch by neurons of the nociceptive lineage is essential for animal survival. Bartesaghi et al. report that the transcriptional regulator PRDM12 is indispensable in neural crest cells (NCCs) for the initiation of the sensory neuronal differentiation program that generates the entire nociceptive lineage.

Highlights

- PRDM12 is expressed in neural crest cells (NCCs) and all nociceptive lineage neurons
- Inactivation of PRDM12 results in the absence of the entire nociceptive lineage
- Forced expression of PRDM12 in NCCs represses non-nociceptor fates
- PRDM12 regulates progenitor proliferation and the sensory neurogenesis program

Bartesaghi et al., 2019, Cell Reports *26*, 3484–3492
March 26, 2019 © 2019 The Author(s).
https://doi.org/10.1016/j.celrep.2019.02.098

CellPress

OPEN ACCESS
CellPress

Cell Reports
Report

PRDM12 Is Required for Initiation of the Nociceptive Neuron Lineage during Neurogenesis

Luca Bartesaghi,[1,2,11] Yiqiao Wang,[1,11] Paula Fontanet,[1] Simone Wanderoy,[1] Finja Berger,[1,2] Haohao Wu,[1] Natalia Akkuratova,[3,4] Filipa Bouçanova,[1,2] Jean-Jacques Médard,[1,2] Charles Petitpré,[1] Mark A. Landy,[5] Ming-Dong Zhang,[6] Philip Harrer,[7] Claudia Stendel,[7] Rolf Stucka,[7] Marina Dusl,[7] Maria Eleni Kastriti,[3,8] Laura Croci,[8] Helen C. Lai,[5] Gian Giacomo Consalez,[9] Alexandre Pattyn,[10] Patrik Ernfors,[6] Jan Senderek,[7] Igor Adameyko,[3,8] Francois Lallemend,[1,12,*] Saida Hadjab,[1,12,13,*] and Roman Chrast[1,2,12,*]

[1]Department of Neuroscience, Karolinska Institutet, Stockholm, 17165, Sweden
[2]Department of Clinical Neuroscience, Karolinska Institutet, Stockholm, 17165, Sweden
[3]Department of Physiology and Pharmacology, Karolinska Institutet, Stockholm, 17165, Sweden
[4]Institute of Translational Biomedicine, Saint Petersburg State University, St. Petersburg, 199034, Russia
[5]Department of Neuroscience, UT Southwestern Medical Center, 5323 Harry Hines Boulevard, Dallas, TX 75390, USA
[6]Department of Medical Biochemistry and Biophysics, Division of Molecular Neurobiology, Karolinska Institutet, Stockholm, 17165, Sweden
[7]Friedrich-Baur-Institute at the Department of Neurology, University Hospital, LMU Munich, Munich, Germany
[8]Center for Brain Research, Medical University Vienna, Vienna, Austria
[9]Università Vita-Salute San Raffaele, 20132, Milan, Italy
[10]Institute for Neurosciences of Montpellier, INSERM, UMR1051, Hôpital Saint-Eloi, Montpellier, 34000, France
[11]These authors contributed equally
[12]These authors contributed equally
[13]Lead Contact
*Correspondence: francois.lallemend@ki.se (F.L.), saida.hadjab@ki.se (S.H.), roman.chrast@ki.se (R.C.)
https://doi.org/10.1016/j.celrep.2019.02.098

SUMMARY

The sensation of pain is essential for the preservation of the functional integrity of the body. However, the key molecular regulators necessary for the initiation of the development of pain-sensing neurons have remained largely unknown. Here, we report that, in mice, inactivation of the transcriptional regulator PRDM12, which is essential for pain perception in humans, results in a complete absence of the nociceptive lineage, while proprioceptive and touch-sensitive neurons remain. Mechanistically, our data reveal that PRDM12 is required for initiation of neurogenesis and activation of a cascade of downstream pro-neuronal transcription factors, including NEUROD1, BRN3A, and ISL1, in the nociceptive lineage while it represses alternative fates other than nociceptors in progenitor cells. Our results thus demonstrate that PRDM12 is necessary for the generation of the entire lineage of pain-initiating neurons.

INTRODUCTION

Two principally different neuron types govern somatosensation: A-fiber low-threshold mechanoreceptors (A-LTMRs) that convey proprioception and touch sensation and the nociceptive lineage, which conveys thermal, pain, and itch sensation. These are specialized peripheral sensory neurons derived from neural crest cells and characterized during development by expression of tropomyosin receptor kinase A (TRKA; gene *Ntrk1*) in the nociceptive lineage and TRKC, TRKB, or RET in A-LTMR lineage (Lallemend and Ernfors, 2012). Although the molecular programs that govern the identities of distinct subtypes of nociceptive neurons are beginning to be understood (Lallemend and Ernfors, 2012), the genetic mechanisms necessary for initiating the lineage of nociceptors remain largely unknown. We have recently identified the transcriptional regulator *PRDM12* to cause congenital insensitivity to pain in humans, but there is limited insight into why it causes a failure of pain perception (Chen et al., 2015). PRDM12 is a transcriptional regulator belonging to the PRDM (PRDI-BF1 and RIZ homology domain) family of putative histone methyltransferases (HMTs) (Hohenauer and Moore, 2012). Members of this family play a role in developmental contexts, including neurogenesis, by driving and maintaining cell state transitions as well as by activating or repressing certain developmental signaling cascades (Matsukawa et al., 2015; Thélie et al., 2015).

We previously observed that in mice, *Prdm12* starts to be detectable around embryonic day 9 (E9) in the neural folds and is strongly expressed in the dorsal root ganglia (DRG) around E10.5 (Chen et al., 2015). These data, together with the observed expression of *PRDM12* during sensory neuron differentiation from induced pluripotent stem cells (iPSCs) and its role in sensory placode development in *Xenopus*, indicated that PRDM12 might participate in sensory neuron development (Chen et al., 2015). Here we use a combination of loss- and gain-of-function approaches in mouse and chicken and demonstrate that PRDM12 is essential for determining specifically the nociceptive lineage from neural crest cell progenitors.

This is an open access article under the CC BY-NC-ND license (http://creativecommons.org/licenses/by-nc-nd/4.0/).

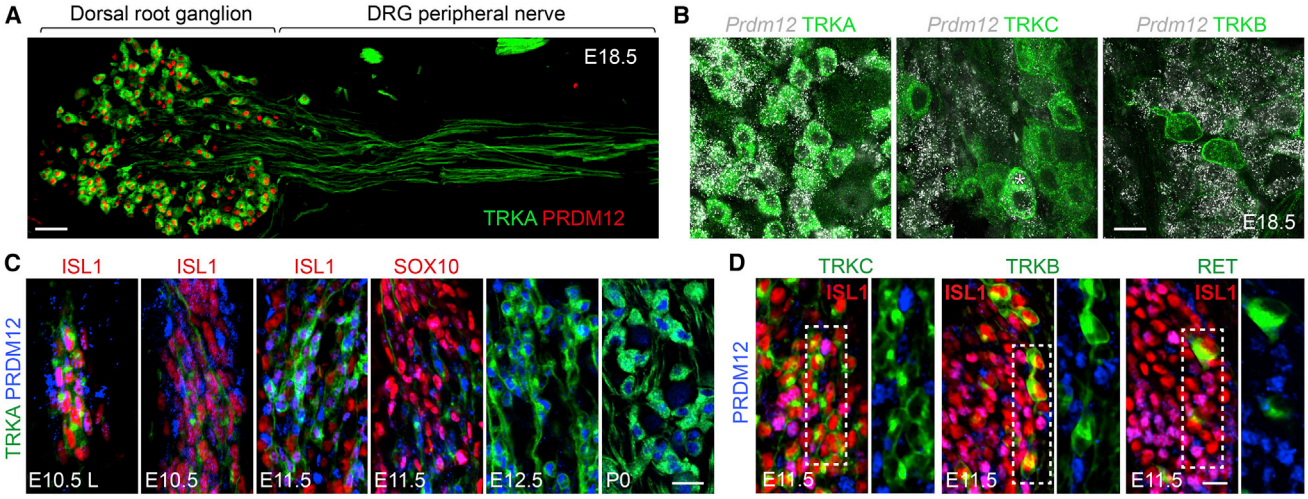

Figure 1. PRDM12 Expression Pattern in the Developing Dorsal Root Ganglia

(A) PRDM12 is present in all TRKA$^+$ nociceptive neurons in the DRG at E18.5 and is not expressed in satellite cells or Schwann cells along the nerve. Scale bar, 50 μm.

(B) *Prdm12* transcript, recognized by *in situ* hybridization, is present in all TRKA$^+$ nociceptive neurons, in very limited number of TRKC$^+$ proprioceptive neurons (asterisk), and in no TRKB$^+$ mechanoreceptors in control mice at E18.5. Scale bar, 20 μm.

(C) During early phases of neurogenesis (E10.5–E11.5), PRDM12 is expressed in early ISL1$^+$/TRKA$^+$ nociceptive neurons and in ISL1$^-$ (and SOX10$^+$) glial and/or precursor cells. PRDM12 is never found outside the DRG. Starting from E12.5, its expression becomes circumscribed to TRKA$^+$ nociceptive neurons. Scale bar, 20 μm.

(D) Immunohistochemistry analysis on E11.5 DRG sections reveals complete absence of PRDM12 expression in A-LTMRs (TRKC$^+$, TRKB$^+$, and RET$^+$). Scale bar, 20 μm.

RESULTS

We investigated the expression pattern of PRDM12 in the mouse DRG using a combination of RNAscope-based *in situ* hybridization and immunohistochemistry approaches. In E18.5 DRG, we observed that the expression of PRDM12 specifically coincided with that of the nociceptive lineage marker TRKA but was largely absent in A-LTMR lineage and in peripheral glial cells (Figures 1A and 1B). Characterization of the developmental profile of PRDM12 expression showed that prior to neurogenesis, it is expressed in SOX10$^+$ precursor cells (Figure 1C). After neurogenesis, PRDM12 is restricted to neurons of the nociceptive lineage (Figures 1B, 1C, S1A) and is absent from all A-LTMRs (marked by expression of TRKC, TRKB, or RET) (Figures 1B–1D). To characterize the role of PRDM12 in sensory neurogenesis, we analyzed two mouse lines with disrupted PRDM12 function: *Prdm12*$^{-/-}$ and *Prdm12*$^{LZ/LZ}$ (Figures S1B–S1E). Successful inactivation of *Prdm12* was confirmed by qPCR, RNAscope-based *in situ* hybridization, and immunohistochemistry (Figures S1E–S1G). Although embryos missing PRDM12 did not present any obvious alteration in their gross morphology (Figure S1D) and survived until very late embryonic development (E18.5), we failed to detect any *Prdm12*$^{-/-}$ or *Prdm12*$^{LZ/LZ}$ newborn pups, indicating perinatal lethality. Interestingly, we observed that the absence of PRDM12 led to a large reduction in the number of NEUN$^+$ neurons and a complete loss of TRKA$^+$ neurons in developing DRG and smaller DRG size (Figures 2A, 2B, and S2A–S2C). Because both *Prdm12*$^{-/-}$ and *Prdm12*$^{LZ/LZ}$ embryos were indistinguishable in terms of inactivation of the *Prdm12* gene (Figures S1E and S1F), sensory ganglia morphology, loss of *Ntrk1* expression (mRNA levels in DRG, normalized to wild-type [WT], expressed as mean ± SD: WT, 1 ± 0.39; *Prdm12*$^{-/-}$, 0.004 ± 0.003; *Prdm12*$^{LZ/LZ}$, 0.0018 ± 0.0006; $p < 0.0005$), and TRKA immunostaining (no TRKA$^+$ cells in both genotypes), we used embryos generated from both lines for the following characterization of the consequences of the loss of PRDM12 function (labeled *Prdm12*$^{-/-}$). Consistent with the reduced DRG size, the total number of ISL1$^+$ neurons was decreased by ~70% at E12.5 in *Prdm12*$^{-/-}$ DRG (Figure 2F). In contrast, the number of A-LTMRs was left unchanged and appeared to be denser than controls as a result of an overall reduction of neurons in the DRG (Figures 2C–2F). This indicates that the absence of TRKA$^+$ cells is not compensated by an increased number of A-LTMRs. Detailed examination of the distinct populations of A-LTMRs indicated a small increase in proprioceptive marker TRKC expression, together with a marked reduction (~60%) in RET expression at E12.5, while TRKB neurons were relatively spared (Figures 2F and S2I).

The specific role of PRDM12 in the nociceptive lineage was further indicated by the absence of expression of nociceptor-specific markers at E18.5 in DRG neurons, including substance P, calcitonin gene-related peptide (CGRP), and tyrosine hydroxylase (TH) (Figures 2H–2J), while CGRP expression in motor neurons and TH expression in sympathetic ganglia were not affected by *Prdm12* mutation (data not shown). Consistently, color-combined triple staining for all A-LTMRs (TRKC, TRKB, and RET) co-stained with ISL1 revealed that all remaining neurons in *Prdm12*$^{-/-}$ are A-LTMRs and myelinated

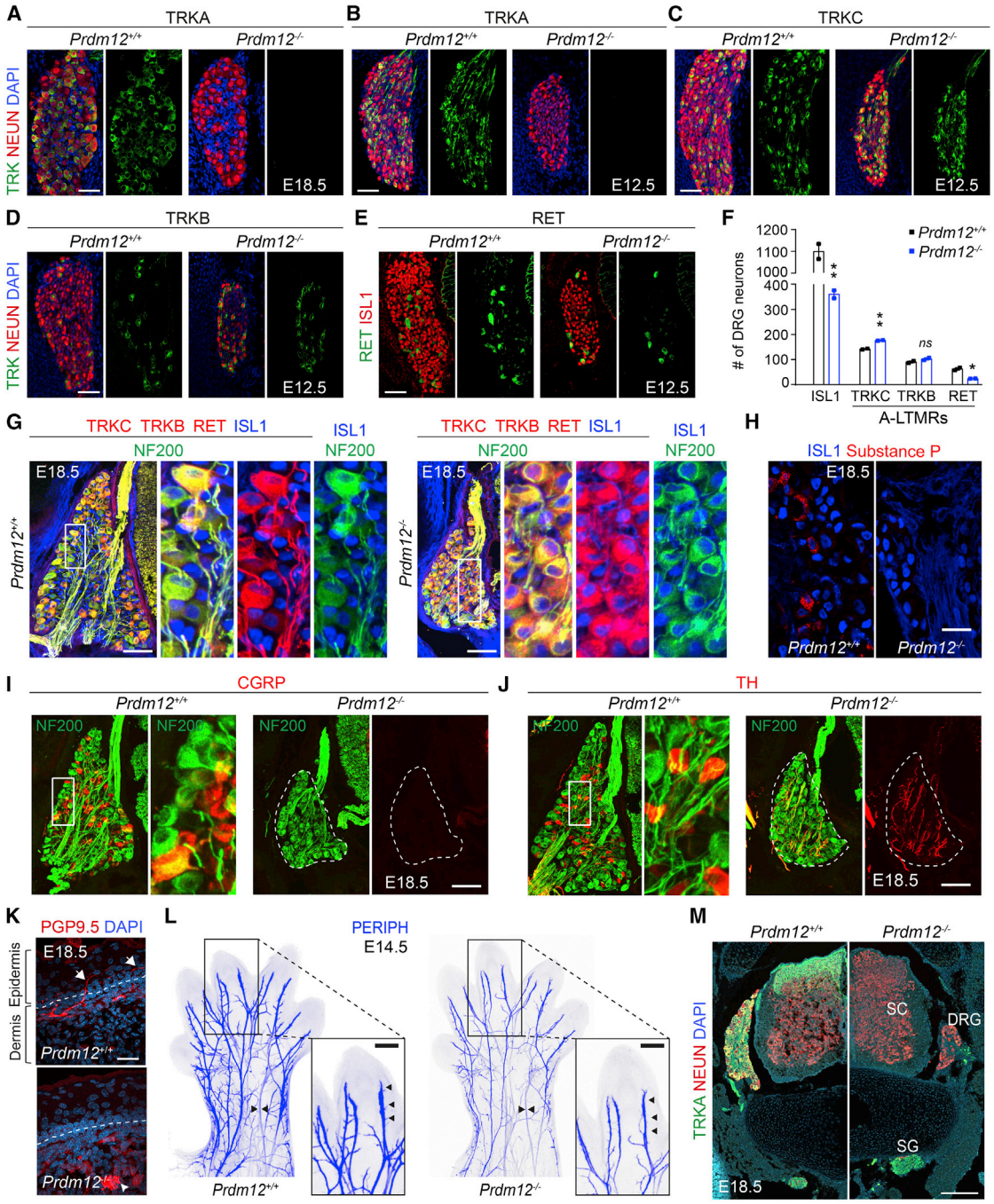

Figure 2. PRDM12 Controls Development of TRKA$^+$ Nociceptors

(A) Immunohistochemistry analysis on E18.5 DRG sections reveals complete absence of nociceptive (TRKA$^+$) neurons in *Prdm12*$^{-/-}$ embryos, leading to reduced size of the DRG. Scale bar, 20 μm.

(B–E) Immunohistochemistry analysis on E12.5 DRG sections confirms the complete absence of nociceptive (TRKA$^+$) neurons in *Prdm12*$^{-/-}$ embryos (B), while A-LTMR (C, TRKC$^+$; D, TRKB$^+$; and E, RET$^+$) populations of neurons are generated in the mutant. Scale bar, 50 μm.

(F) Quantification of neuronal populations on DRG section labeled with ISL1 and TRKC or TRKB or RET. Results are represented in a bar graph and show a 70% decrease in number of neurons in *Prdm12*$^{-/-}$ embryo, while the overall number of A-LTMRs (TRKC$^+$, TRKB$^+$, and RET$^+$) is unchanged. Note that RET number decreases while TRKC increases in *Prdm12*$^{-/-}$ DRG at E12.5. n = 2. *p ≤ 0.05, **p ≤ 0.01; ns, not significant; Student's t test. Data are presented as mean ± SEM.

(G) Combined immunostainings with mixed antibodies for TRKB, TRKC, and RET (red) and NF200 (green), which allows visualization of A-LTMR population co-labeled with ISL1 (blue), show that all neurons observed at E18.5 in the *Prdm12*$^{-/-}$ are A-LTMR mechanoreceptors. n = 4.

(legend continued on next page)

(NF200$^+$) (Figure 2G). The absence of *Prdm12* is marked by loss of sensory epidermis innervation by nociceptors (Figure 2K) and a global reduction of limb innervation accompanied by defects in the small cutaneous sensory nerves (Figures 2L and S2D). In contrast, central and peripheral innervation of proprioceptive neurons (Figures S2E and S2F) and Schwann cell morphology were not affected by PRDM12 deficiency (Figure S2G). The absence of PRDM12 led to a loss of TRKA$^+$ cells also in trigeminal ganglia (Figure S2H), indicating its requirement for the nociceptive lineage also in neurons terminating in the head and neck, but it did not affect TRKA expression in neurons of the sympathetic ganglion (Figure 2M), nor did it affect its size (Figure S2J).

The observed absence of the nociceptive lineage in DRG induced by loss of PRDM12 function may be a consequence of cell death or altered proliferative capacity of neural crest cell derived SOX10$^+$ precursor cells (Kim et al., 2003). We failed to detect any major changes in the number of SOX10$^+$ cells at either E10.5 or E11.5 but could detect a significant decrease at E12.5 (Figure 3A). In contrast, the number of dying SOX10$^+$ precursors (positive for cleaved caspase-3) was invariant between genotypes during the same period (Figure 3A). We then evaluated the proliferative capacity of SOX10$^+$ precursor cells by phospho-histone H3 (pH3) staining, which marks proliferating cells only in late G2 and M phase, leading to relatively small numbers of labeled cells compared with whole cycling population. Although there was no change in the number of pH3$^+$ cells at E10.5, we observed a reduced number of pH3$^+$/SOX10$^+$ cells at E11.5 and E12.5 (Figure 3B).

In order to evaluate if the expression of PRDM12 in neuronal precursor cells is sufficient to initiate the nociceptive lineage, we electroporated chicken embryos at Hamburger and Hamilton stage 13 (HHst13; before neural crest migration) with plasmids expressing a FLAG-tagged PRDM12 or eGFP as a control (Figure 3C). This strategy allows fate tracing of neural crest-derived cells overexpressing PRDM12 or eGFP, as control. Both constructs led to efficient ectopic overexpression at HHst29–30 (~4 days post-electroporation; Figure 3C). In eGFP controls, both glial and neuronal cells in the DRG as well as in cells along nerves were traced (Figures 3D and S3A). Within the DRG, eGFP traced cells included both the TRKA- and TRKC-expressing neurons (Figures 3E and 3F). In contrast, in the periphery, FLAG-PRDM12$^+$ cells were never observed outside the DRG, and all exhibited a neuronal identity (Figures 3D and S3A), with some expressing TRKA (Figure 3E). No PRDM12-overexpressing neurons adopted a TRKC$^+$ (Figure 3F) or TRKB$^+$ (Figure S3B) neuronal identity. However, the percentage of TRKA$^+$ traced neurons remained the same in FLAG-PRDM12$^+$ and eGFP$^+$ (Figure 3E), indicating that PRDM12 is sufficient by itself to repress an A-LTMR fate but is not sufficient to induce TRKA$^+$ neurons. Figure 3G summarizes the results from the gain- and loss-of-function experiments.

Previous work indicated that nociceptors are generated in two waves of neurogenesis, the first, driven by neurogenin 2 (NGN2), which generates A-LTMRs and a small fraction of TRKA$^+$ neurons (early TRKA [eTRKA]), and the second driven by NGN1, which generates the majority of TRKA$^+$ nociceptive lineage (late TRKA [lTRKA]) (Bachy et al., 2011; Hadjab et al., 2013; Lallemend and Ernfors, 2012; Ma et al., 1999). Interestingly, although NGN2 and NGN1 are critical for neurogenesis in the early and late waves of neurogenesis, this requirement reflects timing of expression rather than different instructive functions of NGN1 and NGN2 (Ma et al., 1999). These genes can therefore be used in fate-tracing experiments to determine if PRDM12 is expressed in early- and/or late-born sensory neurons. Reporter mice expressing tdTomato or YFP under the control of either *Ngn1* or *Ngn2* promoters confirmed that eTRKA neurons indeed originate from the NGN2-dependent neurogenesis wave (Florio et al., 2012), while NGN1 drives the development of the lTRKA neurons (Figures 4A–4C). RNAscope *in situ* hybridization indicated that the vast majority of NGN1-wave of neurogenesis expressed PRDM12. Note that a small fraction of the lTRKA neurons were derived from mixed NGN2/NGN1-positive progenitors (10% of YFP$^+$ neurons in $Ngn2^{CreERT2}$;$R26^{YFP}$ DRG were lTRKA neurons; Figures 4A–4C). In support, few *Ngn1*$^+$ neuronal precursor cells were positive for *Ngn2* and for *Prdm12* in the developing DRG at E10.5 (Figure 4D). In the absence of PRDM12, the number of *Ngn2*$^+$ cells was not significantly affected (both at E10.5 and at E10.5 lumbar, which physiologically resembles an E9.5 brachial) (Figure 4D), confirming a normal neurogenesis of the vast majority of neurons in the first wave (A-LTMRs). In contrast, while *Ngn1* was induced at E10.5 (Figure 4E), its expression was almost absent at E12.5 in the mutant DRG (Figures 4F and 4G). This indicates that neurogenin expression in the nociceptive lineage is independent of PRDM12 but rapidly requires PRDM12 for its maintenance. We then tested if *Prdm12* expression can be affected by neurogenins using $Ngn2^{-/-}$ and $Ngn1^{-/-}$ mice (Figures 4I and 4J) and found that *Prdm12* expression is independent of neurogenins. Neurogenins have been shown to act as neuronal determination genes, by activating a cascade of pro-neural genes essential for neuronal commitment and differentiation (Fode et al., 1998; Ma et al., 1998). In the sensory neuron lineage, NEUROD, BRN3A, and ISL1

(H–J) Specific markers of nociceptive neurons (H, substance P; I, CGRP; and J, TH) are not expressed in $Prdm12^{-/-}$ DRG neurons. n = 4.

(K) In the epidermis, sensory nerve endings stained by PGP9.5 are detectable in $Prdm12^{+/+}$ embryos (white arrows) and are absent in $Prdm12^{-/-}$ embryos at E18.5. Arrowhead in $Prdm12^{-/-}$ section indicates Meissner corpuscle (innervated by A-LTMR subtype). Dotted lines indicate boundary between epidermis and dermis. n = 3. Scale bar, 20 μm.

(L) Whole-mount of forelimbs using peripherin (PERIPH) immunolabeling at E14.5 reveals a general decrease in limb innervation (arrowheads point to the same nerve in $Prdm12^{+/+}$ and $Prdm12^{-/-}$ embryos). Insets show higher magnification of digit innervation; arrowheads indicate reduced nerve branching in $Prdm12^{-/-}$ embryos. n = 3. Scale bar, 100 μm.

(M) While TRKA$^+$ neurons in DRG and their projections in spinal cord (SC) are absent in $Prdm12^{-/-}$ embryos at E18.5, TRKA expression in sympathetic ganglia (SG) is not affected. n = 3. Scale bar, 200 μm.

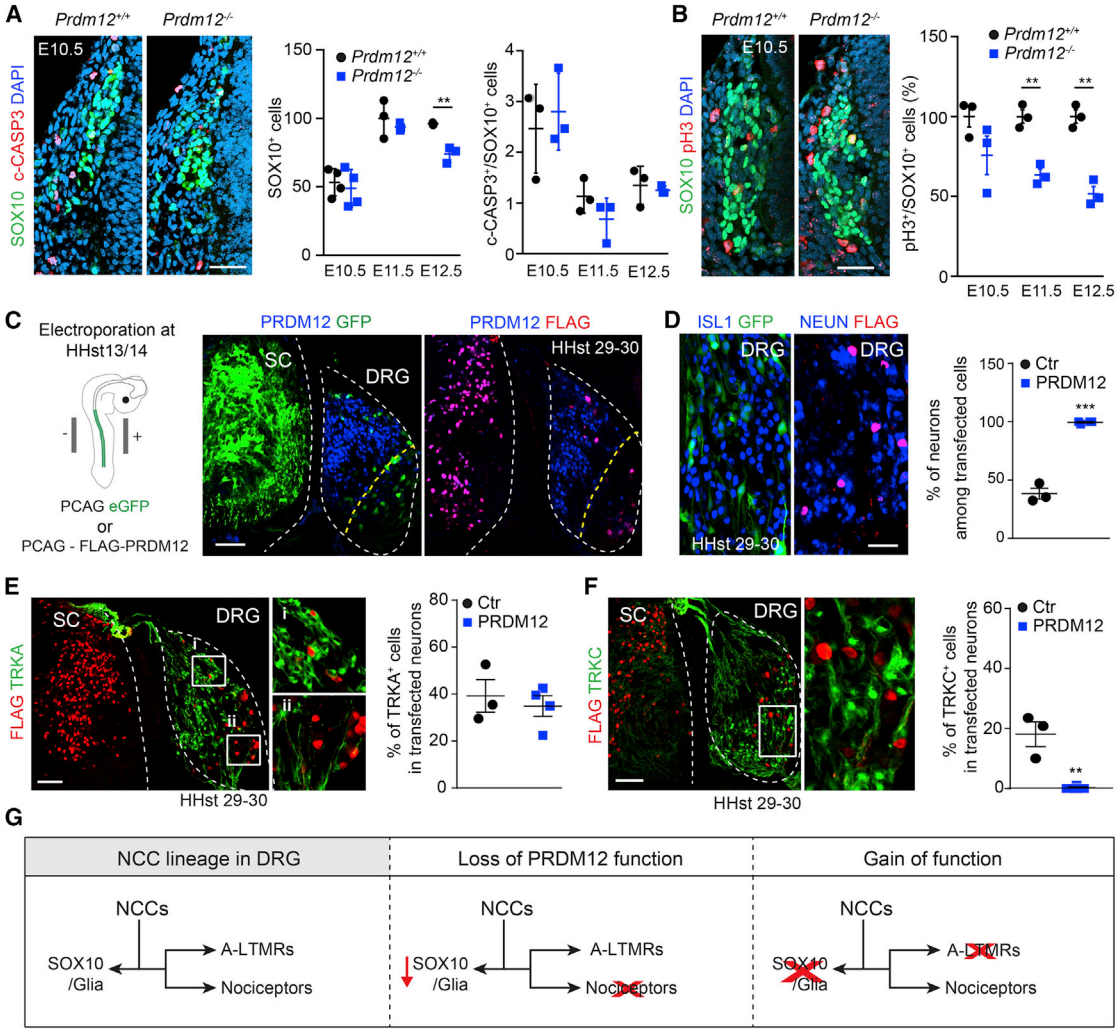

Figure 3. Ectopic Expression of PRDM12 Specifies Neural Crest Cells for a Sensory Neuron Fate and Represses TRKC

(A and B) DRG sections obtained from *Prdm12*$^{-/-}$ and *Prdm12*$^{+/+}$ E10.5 embryos immunostained for (A) SOX10 and cleaved caspase-3 (c-CASP3; labels apoptotic cells) and (B) SOX10 and the mitosis-specific marker phospho-histone-3 (pH3). Scale bars, 50 μm. Graphs show quantification of the immunostainings and reveal no change in the proportion of cell death within the precursors cell population (c-CASP3$^+$/SOX10$^+$) in *Prdm12*$^{-/-}$ mice (A) but a decrease in the number of proliferative SOX10$^+$ cells at both E11.5 and E12.5 in mutant mice (B) (stages earlier than E10.5 have not been analyzed). n = 3; **p ≤ 0.01 (Student's t test). Data are presented as mean ± SEM.

(C) Gain of function (overexpression) of PRDM12 in neural crest cells using *in ovo* electroporation of pCAG-FLAG-PRDM12 (PRDM12 condition) plasmid at HHst13/14 or of the control plasmid pCAG-eGFP (control [Ctr] condition). Sections of electroporated HHst29–30 embryos are shown, immunostained for PRDM12 and endogenously expressing GFP fluorescence or immunostained for PRDM12 and FLAG. HHst29–30 corresponds to ~E13.5 in mouse development. Successful electroporation is seen by expression of the reporter GFP or FLAG in both half of the neural tube and DRG cells (GFP, n = 3, an average of 180 electroporated DRG cells were analyzed per embryo; FLAG, n = 4, an average of 74 electroporated DRG cells were analyzed per embryo). PRDM12 immunostaining is present in the dorso-medial region of the DRG in chicken, corresponding to the nociceptor population. Scale bar, 50 μm.

(D) Analysis of neuronal markers (ISL1 and NEUN) in the Ctr and PRDM12 conditions reveals a complete absence of non-neuronal cells in FLAG$^+$ cells, while both neuronal and glial cells (ISL1$^-$) are represented among GFP-positive cells. Graph shows quantification of the immunostainings. ***p ≤ 0.001 (Student's t test). Data are presented as mean ± SEM. Scale bar, 25 μm.

(E and F) Quantification of the TRKA$^+$ cells (E) and TRKC$^+$ cells (F) among transfected neurons in DRG reveals a complete lack of TRKC expression in the PRDM12 condition (n = 4), while it represents 19% of the GFP$^+$ neurons in the Ctr condition (n = 3). **p ≤ 0.01 (Student's t test). Data are presented as mean ± SEM. Scale bar, 50 μm.

(G) Representative scheme of the experiment outcome.

are sequentially expressed following expression of neurogenins (Fode et al., 1998; Ma et al., 1999; Marmigère and Ernfors, 2007; Montelius et al., 2007; Sommer et al., 1996). In line with the neurogenin defect, the expression of these transcription factors in DRG were sharply reduced in *Prdm12*$^{-/-}$ mutant embryos, as revealed by qPCR (Figure 4G), and

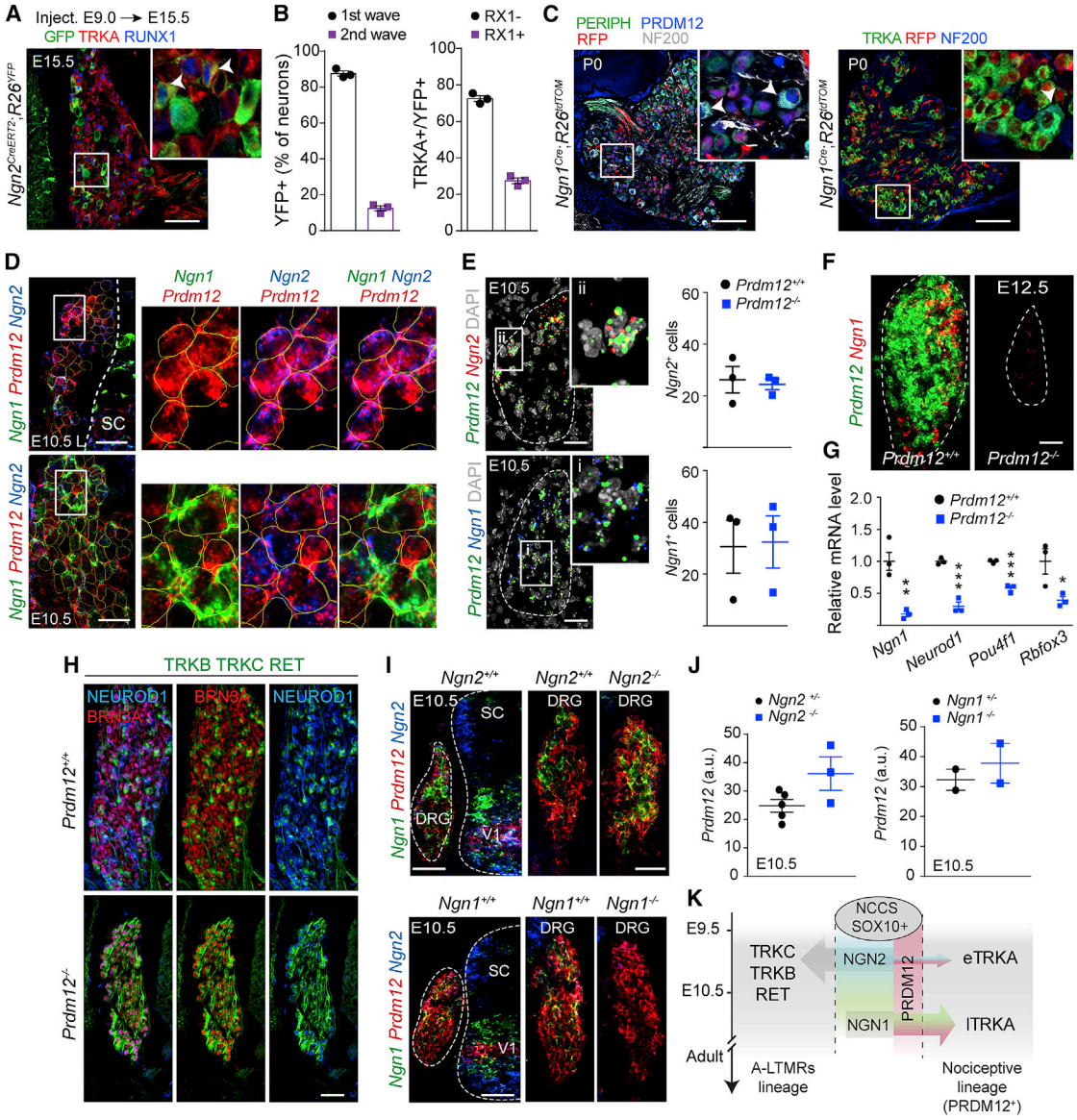

Figure 4. PRDM12^{+} Nociceptors Are Generated From Two Neurogenic Waves, and PRDM12 Controls Neurogenesis of the Nociceptive Lineage

(A) Lineage tracing of sensory neurons progenitors using *Ngn2$^{CreERT/+}$;R26^{YFP}* mice. Tamoxifen was injected at E9, and the embryos were harvested at E15.5. DRG sections were immunostained for GFP (to label YFP), TRKA, and RUNX1 expression. Inset represents higher magnification of selected area. Arrowheads indicate traced nociceptor neurons from the second wave identified as YFP^{+}/RUNX1^{+}/TRKA^{+}. Nociceptive neurons of the first wave are RUNX1 negative (Gascon et al., 2010). Scale bar, 60 μm.

(B) Quantification of first wave-born versus second wave-born nociceptor neurons identified by YFP^{+}/TRKA^{+}/RUNX1^{-} and YFP^{+}/TRKA^{+}/RUNX1^{+}, respectively. The quantification revealed that NGN2 lineage traced cells (YFP^{+}) give rise to ~10% of second-wave neurons; thus, among nociceptive neurons ~75% of traced cells are first wave and ~25% are second wave in our *Ngn2*-dependent genetic tracing (n = 3).

(C) Lineage tracing of sensory neurons progenitors using *Ngn1^{Cre};R26^{tdTOM}* mice. Brachial DRG sections of P0 mice were immunostained for peripherin (PERIPH), PRDM12, RFP, NF200, and TRKA expression and show 100% recombination among second-wave nociceptive neurons, while neurons from the first wave, including eTRKA nociceptors, are negative. Insets represent higher magnification of selected area. Arrowheads indicate first-wave nociceptive neurons (PERIPH^{+}/NF200^{+} or TRKA^{+}/NF200^{+}) negative for RFP. n = 3. Scale bar, 100 μm.

(D) RNAscope of *Prdm12* with *Ngn1* or *Ngn2* on E10.5 lumbar (E10.5L; developmentally equivalent to E9.5 brachial; top) and E10.5 brachial (E10.5; bottom) DRG section (SC [spinal cord]). The *in situ* hybridization reveals the existence of progenitor pool that concomitantly express *Ngn2*, *Prdm12*, and *Ngn1*. Possible interdependency of PRDM12, NGN1, and NGN2 is investigated in (E), (F), and (J). Scale bars, 20 μm.

(E) RNAscope of *Prdm12* with *Ngn1* or *Ngn2* on E10.5 brachial DRG section. Nuclei are counterstained with DAPI. Quantification of the *Ngn1*$^{+}$ and *Ngn2*$^{+}$ cells reveals unchanged number in *Prdm12*$^{-/-}$ compared with *Prdm12*$^{+/+}$ embryos (n = 3). Scale bar, 50 μm.

(F) RNAscope of *Ngn1* performed on E12.5 *Prdm12*$^{+/+}$ and *Prdm12*$^{-/-}$ DRG shows a clear reduction of *Ngn1* expression. n = 3. Scale bar, 50 μm.

(legend continued on next page)

were never found outside the A-LTMR populations (TRKC$^+$, TRKB$^+$, or RET$^+$ neurons; Figure 4H). Altogether, these results indicate that PRDM12 is necessary within the nociceptive lineage, where it is required for maintaining neurogenin expression, which is necessary for neurogenesis and for activating downstream genetic pathways required for overt neuronal differentiation.

In summary, we demonstrate that PRDM12 is critical for progenitor cell proliferation and for the activation of the neurogenic program in neural crest cells that generate the nociceptive lineage regardless of their birthdate (Figure 4K).

DISCUSSION

The sensation of pain is essential for preserving the functional integrity of the body. Yet the molecular mechanisms necessary to drive the development of pain-sensing neurons and to maintain their homeostasis in adults are still largely unknown. Previous studies have demonstrated the importance of *Ngn1* for the generation of a majority of the nociceptive lineage (Ma et al., 1999). However, neurogenin function is not specific to neuron subtypes but to the timing of neurogenesis (Lallemend and Ernfors, 2012; Ma et al., 1999), leaving unresolved the question as to whether specific molecular pathways control the development of specific sensory neuron types from precursor cells. Here we demonstrate that PRDM12 is essential for determining nociceptive sensory neuron fate from neural crest cell progenitors. Importantly, in the absence of PRDM12, specific neuronal progenitors completely fail to maintain neurogenin expression, to activate that of the pro-neuronal genes NEUROD1, BRN3A, and ISL1, and to develop into nociceptive neurons, while the generation of A-LTMRs from distinct populations of progenitors is generally preserved.

This observation implies early predetermination of subsets of sensory neuron precursors to the nociceptive lineage and suggests the existence of distinct subclones in progenitors. In this context, PRDM12 expression is, however, not limited to nociceptor progenitors, yet its role in neurogenesis is primarily limited to and necessary for the entire nociceptive lineage. This strongly suggests the existence of co-factors or differential molecular landscapes within the nociceptor progenitor lineage that, together with PRDM12, would restrict their neuron fate commitment. Interestingly, the absence of *Prdm12* results in the loss of neurogenin expression concomitant with a decrease in the number of progenitors and of their proliferation. This raises the possibility that PRDM12, through its regulatory function on neurogenin expression, could be necessary for both the expansion of the neuronal progenitor pool and their commitment to sensory neuron lineage. In this context, in the absence of neurogenin function, many progenitors that would normally be restricted to the production of neurons, could remain either undifferentiated or produce glial cells instead. Previous studies in the field have lent support for the latter (i.e., the alternative glial fate; Nieto et al., 2001; Sun et al., 2001). Further understanding of the link between PRDM12 and neurogenins and their downstream cellular functions will be necessary in order to clarify the outcome of the mutant cells, which, in normal conditions, would have developed into TRKA$^+$ neurons. In addition, supplementary insights into the identity of the potential PRDM12 interactors and into the transcriptional and epigenomic changes in sensory neuron progenitors upon *Prdm12* manipulation will be important to understand the breadth of gene regulation by PRDM12 during generation of the nociceptive lineage.

Our findings also show that soon after sensory neurons have become postmitotic, their diversity is already defined by their maintenance of PRDM12 expression in all nociceptive neurons, while other known sensory neuron markers are not yet segregated. This makes PRDM12 the earliest and the only known DNA-binding factor distinguishing neurons of the nociceptive lineage from touch-sensitive mechanoreceptors and proprioceptors. We also demonstrate that forcing expression of PRDM12 alone is not sufficient to drive generation of TRKA$^+$ nociceptors in sensory neurons. Instead, our data suggest that PRDM12 can limit cell fate to sensory neurons in the DRG where, interestingly, it represses alternative fate other than nociceptor in postmitotic cells.

Hence, our study demonstrates that the mechanism of nociceptive fate commitment is molecularly defined in precursors and suggests that the lack of sensitivity to pain observed in patients carrying *PRDM12* gene mutation is likely due to a failure in the generation of pain-sensing neurons. More broadly, this is consistent with the general emerging idea that core aspects of neuron identity are already drafted in progenitors (Franco et al., 2012; Mi et al., 2018). Yet the molecular context in which PRDM12 operates in particular progenitors to specify their presumptive nociceptive fate remains to be identified. Further elucidation of involved molecular mechanisms will provide key insights into how sensory neuron diversity is generated and may provide genetic tools to induce a desired neuronal lineage in stem cell engineering. Finally, the persistently restricted expression of PRDM12 in adult pain-sensing neurons (Usoskin et al., 2015) (Figure S1A) indicates that its regulatory role may also modulate the function of mature neurons of the nociceptive lineage (conveying thermal, pain, and itch sensation), providing a potential target

(G) Relative mRNA expression (by qPCR) for *Ngn1*, *Neurod1*, and *Pou4f1* (coding for BRN3A) and *Rbfox3* (coding for NEUN) mRNAs in E12.5 DRG. Comparison between *Prdm12*$^{+/+}$ and *Prdm12*$^{-/-}$ shows significantly lower expression in mutant samples. n = 3. *p ≤ 0.05, **p ≤ 0.01, and ***p ≤ 0.001 (Student's t test). Data are presented as mean ± SEM.

(H) Immunostaining for NEUROD1 and BRN3A on E12.5 DRG sections reveals their restricted expression in A-LTMR populations (TRKC, TRKB, RET; green) in *Prdm12*$^{-/-}$. n = 2.

(I) RNAscope for *Ngn1*, *Prdm12*, and *Ngn2* on E10.5 brachial DRG sections from *Ngn2*$^{-/-}$ (top) and *Ngn1*$^{-/-}$ (bottom) embryos and their respective control embryos. Scale bars, 80 μm. Higher magnification pictures of DRG area: scale bar, 50 μm.

(J) Quantifications of (I) show no difference in *Prdm12* expression between *Ngn*$^{+/-}$ and *Ngn*$^{-/-}$ animals (n = 2–5).

(K) Scheme recapitulating the role of PRDM12 in the commitment of neuronal precursor cells into the major different sensory neuron fates.

for therapeutic approaches aiming at the modulation of pain perception.

STAR★METHODS

Detailed methods are provided in the online version of this paper and include the following:

- KEY RESOURCES TABLE
- CONTACT FOR REAGENT AND RESOURCE SHARING
- EXPERIMENTAL MODEL AND SUBJECT DETAILS
  - Animals
- METHOD DETAILS
  - Genotyping of mice
  - RNA isolation, RT-PCR and qPCR
  - Immunohistochemistry (IHC)
  - RNAscope® *in situ* hybridization
  - Whole mount Immunofluorescence
  - In ovo electroporation
  - Electron microscopy
- QUANTIFICATION AND STATISTICAL ANALYSIS

SUPPLEMENTAL INFORMATION

Supplemental Information can be found with this article online at https://doi.org/10.1016/j.celrep.2019.02.098.

ACKNOWLEDGMENTS

We thank Prof. Frances Lefcort for anti-chicken TRKA and TRKC antibodies, Prof. Tomas Hökfelt for anti-rabbit CGRP antibody, Prof. Francois Guillemot for the *Ngn*-null mice, the CLICK Imaging Facility supported by the Knut and Alice Wallenberg Foundation, and Prof. Yiochi Shinkai for the pCAG-FLAG-mPRDM12 plasmid. This work was supported by grants from StratNeuro, the Swedish Research Council, and KID funding (F.L. and R.C.); the Knut and Alice Wallenberg Foundation (Wallenberg Academy Fellow), the Swedish Brain Foundation, the Åke Wiberg Foundation, Karolinska Institutet (Faculty Funded Career Position), the Ragnar Söderberg Foundation (Ragnar Söderberg Fellow in Medicine), and a Ming Wai Lau research grant (F.L.); ERC AdvPainCells 740491 and the Knut and Alice Wallenberg Foundation (P.E.); Inserm (A.P.); the Rita Allen Foundation (H.C.L.); the Russian Science Foundation (grant 16-15-10273 to N.A.); the German Federal Ministry of Education and Research (BMBF) through the German Network for Charcot-Marie-Tooth Neuropathies (CMT-NET) (01GM1511B to J.S.); and Fritz-Thyssen-Stiftung (Az. 10.15.1.021MN to J.S. and C.S.) and the LMU FoeFoLe program (36/2014 to J.S.).

AUTHOR CONTRIBUTIONS

F.L., S.H., and R.C. contributed equally, and each has the right to list her or himself last in bibliographic documents. L.B. and Y.W. contributed equally, and each has the right to list himself first in bibliographic documents. F.L., S.H., and R.C. designed and supervised the study. L.B. and Y.W. performed most experiments. R.S., C.S., P.H., M.D., and J.S. generated *Prdm12*$^{-}$ and *Prdm12*^{LZ} alleles. P.F., S.W., F. Berger, H.W., C.P., N.A., F. Bouçanova, J.-J.M., M.-D.Z., and S.H. performed some immunostaining experiments and microscopy analysis. M.A.L., M.E.K., H.C.L., A.P., J.-J.M., P.E., L.C., G.G.C., and I.A. processed and provided mouse tissues for analysis. N.A. performed chicken electroporation. F.L., S.H., and R.C. prepared the figures. F.L., S.H., and R.C. wrote the paper with input from all other authors.

DECLARATION OF INTERESTS

The authors declare no competing interests.

Received: October 12, 2018
Revised: December 6, 2018
Accepted: February 25, 2019
Published: March 26, 2019

REFERENCES

Bachy, I., Franck, M.C., Li, L., Abdo, H., Pattyn, A., and Ernfors, P. (2011). The transcription factor Cux2 marks development of an A-delta sublineage of TrkA sensory neurons. Dev. Biol. *360*, 77–86.

Britz, O., Mattar, P., Nguyen, L., Langevin, L.M., Zimmer, C., Alam, S., Guillemot, F., and Schuurmans, C. (2006). A role for proneural genes in the maturation of cortical progenitor cells. Cereb. Cortex *16* (*Suppl 1*), i138–i151.

Chen, Y.C., Auer-Grumbach, M., Matsukawa, S., Zitzelsberger, M., Themistocleous, A.C., Strom, T.M., Samara, C., Moore, A.W., Cho, L.T., Young, G.T., et al. (2015). Transcriptional regulator PRDM12 is essential for human pain perception. Nat. Genet. *47*, 803–808.

Florio, M., Leto, K., Muzio, L., Tinterri, A., Badaloni, A., Croci, L., Zordan, P., Barili, V., Albieri, I., Guillemot, F., et al. (2012). Neurogenin 2 regulates progenitor cell-cycle progression and Purkinje cell dendritogenesis in cerebellar development. Development *139*, 2308–2320.

Fode, C., Gradwohl, G., Morin, X., Dierich, A., LeMeur, M., Goridis, C., and Guillemot, F. (1998). The bHLH protein NEUROGENIN 2 is a determination factor for epibranchial placode-derived sensory neurons. Neuron *20*, 483–494.

Franco, S.J., Gil-Sanz, C., Martinez-Garay, I., Espinosa, A., Harkins-Perry, S.R., Ramos, C., and Müller, U. (2012). Fate-restricted neural progenitors in the mammalian cerebral cortex. Science *337*, 746–749.

Gascon, E., Gaillard, S., Malapert, P., Liu, Y., Rodat-Despoix, L., Samokhvalov, I.M., Delmas, P., Helmbacher, F., Maina, F., and Moqrich, A. (2010). Hepatocyte growth factor-Met signaling is required for Runx1 extinction and peptidergic differentiation in primary nociceptive neurons. J. Neurosci. *30*, 12414–12423.

Hadjab, S., Franck, M.C., Wang, Y., Sterzenbach, U., Sharma, A., Ernfors, P., and Lallemend, F. (2013). A local source of FGF initiates development of the unmyelinated lineage of sensory neurons. J. Neurosci. *33*, 17656–17666.

Hohenauer, T., and Moore, A.W. (2012). The Prdm family: expanding roles in stem cells and development. Development *139*, 2267–2282.

Kim, J., Lo, L., Dormand, E., and Anderson, D.J. (2003). SOX10 maintains multipotency and inhibits neuronal differentiation of neural crest stem cells. Neuron *38*, 17–31.

Lallemend, F., and Ernfors, P. (2012). Molecular interactions underlying the specification of sensory neurons. Trends Neurosci. *35*, 373–381.

Ma, Q., Chen, Z., del Barco Barrantes, I., de la Pompa, J.L., and Anderson, D.J. (1998). Neurogenin1 is essential for the determination of neuronal precursors for proximal cranial sensory ganglia. Neuron *20*, 469–482.

Ma, Q., Fode, C., Guillemot, F., and Anderson, D.J. (1999). Neurogenin1 and neurogenin2 control two distinct waves of neurogenesis in developing dorsal root ganglia. Genes Dev. *13*, 1717–1728.

Marmigère, F., and Ernfors, P. (2007). Specification and connectivity of neuronal subtypes in the sensory lineage. Nat. Rev. Neurosci. *8*, 114–127.

Matsukawa, S., Miwata, K., Asashima, M., and Michiue, T. (2015). The requirement of histone modification by PRDM12 and Kdm4a for the development of pre-placodal ectoderm and neural crest in Xenopus. Dev. Biol. *399*, 164–176.

Mi, D., Li, Z., Lim, L., Li, M., Moissidis, M., Yang, Y., Gao, T., Hu, T.X., Pratt, T., Price, D.J., et al. (2018). Early emergence of cortical interneuron diversity in the mouse embryo. Science *360*, 81–85.

Montelius, A., Marmigère, F., Baudet, C., Aquino, J.B., Enerbäck, S., and Ernfors, P. (2007). Emergence of the sensory nervous system as defined by Foxs1 expression. Differentiation *75*, 404–417.

Nieto, M., Schuurmans, C., Britz, O., and Guillemot, F. (2001). Neural bHLH genes control the neuronal versus glial fate decision in cortical progenitors. Neuron *29*, 401–413.

Quiñones, H.I., Savage, T.K., Battiste, J., and Johnson, J.E. (2010). Neurogenin 1 (Neurog1) expression in the ventral neural tube is mediated by a distinct

enhancer and preferentially marks ventral interneuron lineages. Dev. Biol. *340*, 283–292.

Sommer, L., Ma, Q., and Anderson, D.J. (1996). Neurogenins, a novel family of atonal-related bHLH transcription factors, are putative mammalian neuronal determination genes that reveal progenitor cell heterogeneity in the developing CNS and PNS. Mol. Cell. Neurosci. *8*, 221–241.

Sun, Y., Nadal-Vicens, M., Misono, S., Lin, M.Z., Zubiaga, A., Hua, X., Fan, G., and Greenberg, M.E. (2001). Neurogenin promotes neurogenesis and inhibits glial differentiation by independent mechanisms. Cell *104*, 365–376.

Thélie, A., Desiderio, S., Hanotel, J., Quigley, I., Van Driessche, B., Rodari, A., Borromeo, M.D., Kricha, S., Lahaye, F., Croce, J., et al. (2015). Prdm12 specifies V1 interneurons through cross-repressive interactions with Dbx1 and Nkx6 genes in Xenopus. Development *142*, 3416–3428.

Usoskin, D., Furlan, A., Islam, S., Abdo, H., Lönnerberg, P., Lou, D., Hjerling-Leffler, J., Haeggström, J., Kharchenko, O., Kharchenko, P.V., et al. (2015). Unbiased classification of sensory neuron types by large-scale single-cell RNA sequencing. Nat. Neurosci. *18*, 145–153.

STAR★METHODS

KEY RESOURCES TABLE

REAGENT or RESOURCE	SOURCE	IDENTIFIER
Antibodies		
GpAb TrkA	R&D Systems	Cat#AF1056, AB_2283049
GpAb TrkB	R&D Systems	Cat#AF1494, AB_2155264
GpAb TrkC	R&D Systems	Cat#AF1404, AB_2155412
RpAb TrkC	Cell Signaling	Cat#3376S, AB_2155283
GpAb RET	R&D Systems	Cat#AF482, AB_2301030
RpAb CGRP	From T. Hökfelt	N/A
Rbt NeuN (D4G4O) XP®	Cell Signaling Technology	Cat#24307, AB_2651140
RpAb Prdm12	Sigma – Aldrich	Cat#HPA043143, AB_10806379
MmAb Isl1	Developmental Studies Hybridoma Bank	Cat#39.4D5, AB_2314683
MmAb Sox10	From I. Adameyko	N/A
RpAb Sox10 (D5V9L)	Cell Signaling	Cat#89356S; RRID:AB_2792980
RpAb TH	Pel-Freez	Cat#P40101, AB_2313713
Peripherin	Millipore	Cat#AB1530, AB_90725
Pgp9.5	Cedarlane	Cat#CL7756AP; RRID:AB_2792979
NF-200	Sigma – Aldrich	Cat#N0142, AB_477257
ChkpAb NF200	Abcam	Cat#ab4680, AB_304560
Phalloidin	Molecular probes	Cat#A12379, AB_2315147
Neurofilament 165 (2H3)	DSHB, University of Iowa	AB_531793
PEA3	From S. Arber	AB_2631976
Parvalbumin	Swant	Cat#PV-28, AB_2315235
RmAb Flag M2	Sigma – Aldrich	Cat#F1804, AB_262044
TrkA (for chicken exp)	From F. Lefcort and P. Ernfors	AB_2315490
TrkC (for chicken exp)	From F. Lefcort and P. Ernfors	AB_2315492
RpAb Cleaved Caspase 3	Cell Signaling	Cat#9664, AB_2070042
RpAb phospho-histone 3 (pHis3)	Millipore	Cat#06-570, AB_310177
ChkpAb GFP	Abcam	Cat#AB13970, AB_300798
RpAb Runx1	From T. Jessel	N/A
Bacterial and Virus Strains		
One Shot TOP10	Invitrogen	Cat#C404003
Chemicals, Peptides, and Recombinant Proteins		
SYBR® Green Master (ROX)	F. Hoffmann-La Roche	Cat#28137500
NEG-50	Thermo Fisher Scientific	Cat#6502Y
DAPI	Sigma	Cat#10236276001
VECTASHIELD	Vector Laboratories	Cat#H-1000 AB_2336789
RNAscope probe Mm-Prdm12	ACDBio	Cat#524371
RNAscope probe Mm-Neurog1	ACDBio	Cat#414211
RNAscope probe Mm-Neurog2	ACDBio	Cat#417291
RNAscope Fluorescent Multiplex	ACDBio	Cat#320850
RNAscope Multiplex Fluorescent v2	ACDBio	Cat#323100
TSA Plus Fluorescin Evaluation Kit	Perkin Elmer	Cat#NEL741E001KT
TSA Plus Cyanine 3 System	Perkin Elmer	Cat#NEL744E001KT
TSA Plus Cyanine 5 System	Perkin Elmer	Cat#NEL745E001KT

(*Continued on next page*)

Continued		
REAGENT or RESOURCE	SOURCE	IDENTIFIER
Critical Commercial Assays		
QIAzol® Lysis Reagent	QIAGEN	Cat#79306
RNeasy® Lipid Tissue Mini Kit	QIAGEN	Cat#74804
PrimeScript RT reagent kit	Takara Bio Inc	Cat#RR037A
DreamTaq Green PCR MasterMix (2x)	Thermo Scientific	Cat#K1081
Experimental Models: Organisms/Strains		
Mouse: C57BL/6N Prdm12 < tm2a(EUCOMM) Hmgu > /Tcp	CMMR	Code: ABIJ
Mouse: *Prdm12$^{LZ/LZ}$*	This paper	N/A
Mouse: *Prdm12$^{-/-}$*	This paper	N/A
Mouse: *Gt(ROSA)26Sor$^{tm1(ACTB-cre,\ -EGFP)Ics}$*	ICS, Illkirch, France	N/A
Mouse: Tg(CAG-flpe)2Arte	Taconic	Taconic: Cat#7089
Mouse: *Ngn1^{Cre}* (named N1 457-Cre)	Quiñones et al., 2010	N/A
Mouse: *Ngn2^{creERT2}*	Florio et al., 2012	N/A
Mouse: *Ngn1$^{-/-}$*	Ma et al., 1999	N/A
Mouse: *Ngn2$^{-/-}$* (named Ngn2KIGFP)	Britz et al., 2006	N/A
Chicken: white Leghorn eggs	OVA Production AB	N/A
Oligonucleotides		
Primers for genotyping, see Table S1	This paper	N/A
Primers for qPCR, see Table S1	This paper	N/A
Recombinant DNA		
pCAGeGFP	Generated by F. Lallemend	N/A
pCAG-FLAG-mPRDM12-IRES-puro	Gift from Y. Shinkai	N/A

CONTACT FOR REAGENT AND RESOURCE SHARING

Further information and requests for resources and reagents should be directed to and will be fulfilled by the Lead Contact, Saida Hadjab (Saida.Hadjab@ki.se).

EXPERIMENTAL MODEL AND SUBJECT DETAILS

Animals

Mice

Prdm12$^{LZ/LZ}$ and *Prdm12$^{-/-}$* mice were generated by crossing *Prdm12$^{tm2a/+}$* strain obtained from the Canadian Mouse Mutant Repository (CMMR, Toronto, Canada) with Cre deleter mice *Gt(ROSA)26Sor$^{tm1(ACTB-cre,\ -EGFP)Ics}$* from ICS (Illkirch, France) and with Flp deleter mice Tg(CAG-flpe)2Arte from Taconic (Model # 7089) leading to generation of the *Prdm12^{LZ}* allele, where exon 2 of the *Prdm12* gene has been replaced by LacZ ORF, and to the *Prdm12^{-}* allele where exon 2 is fully deleted (Figure S1B). *Ngn1^{Cre} mice* samples were obtained from Helen Lai, *Ngn1$^{-/-}$* and *Ngn2$^{-/-}$* mice samples have been previously described and were obtained from Alexandre Pattyn. *Ngn2^{creERT2}* samples were obtained from Giacomo G. Consalez.

Chicken

Fertile white Leghorn eggs were incubated at 38°C and embryos were staged according to Hamburger-Hamilton (HH) tables. In our experiments, embryonic day (E) 2 and 6 correspond to Hamburger and Hamilton stages 13, and 29-30 respectively.

Animals of either sex were included in this study. Animals were group-housed, with food and water *ad libitum,* under 12hr light-dark cycle conditions. All animal work was performed in accordance with the Swedish regulations and approved by the regional ethics review committee Stockholm, Stockholms norra djurförsöksetiska nämnd.

METHOD DETAILS

Genotyping of mice

Genomic DNA extracted from ear or tail biopsies was used to determine the genotype of each mouse. DreamTaq Green Master Mix was used to perform the amplification (35 cycles with an annealing temperature of 59°C). The primers used for the genotyping PCR are listed in Table S1 and their position is indicated in Figure S1B.

RNA isolation, RT-PCR and qPCR

DRGs were collected from mutant and wild-type animals at E12.5 from both Prdm12 lines (*Prdm12*$^{+/+}$, *Prdm12*$^{+/-}$, *Prdm12*$^{-/-}$, *Prdm12*$^{+/LZ}$ *and Prdm12*$^{LZ/LZ}$). mRNA was isolated using the RNeasy® Lipid Tissue Mini Kit (QIAGEN, Hilden, Germany), following the manufacturer's instructions. Tissue was homogenized in QIAzol® Lysis Reagent using a TissueLyser II and optional DNase digestion was performed according to the RNeasy® Lipid Tissue Handbook (QIAGEN). Reverse transcription (RT)-PCR was performed using PrimeScript RT reagent kit manual (Takara Bio Inc., Kusatsu, Japan) employing equal amounts of RNA among samples. qPCR was performed based on the SYBR® Green System (F. Hoffmann-La Roche AG, Basel, Switzerland) using the Applied Biosystems 7500 Real-Time PCR System (Thermo Fisher Scientific, Inc.). Relative mRNA expression of *TrkA/Ntrk1*, *Ngn1, Neurod1, Pou4f1, Rbfox3*, and *Prdm12* were analyzed. The obtained expression levels were normalized using the expression of *Actb* as reference gene (the *Prdm12*$^{+/+}$ values for normalized mRNA expression of each gene were arbitrarily set to 1).

Immunohistochemistry (IHC)

Embryos were collected, decapitated and fixed in 4% paraformaldehyde (PFA) in PBS for 1-6hrs (depending on the stage) at 4°C, washed in PBS, cryopreserved in 30% sucrose in PBS and subsequently embedded in NEG-50 (Thermo Fisher Scientific, Inc.). Cryosections were collected onto Superfrost Plus slides at 14 μm thickness. Sections were washed in PBS prior to incubation in blocking solution (5% BSA, 1% normal donkey serum, 0.02% NaAz in PBS or 2% donkey serum, 0.5% Triton X-100 in PBS) for 1h at room temperature (RT). Nuclei were counterstained with DAPI (1:10.000 in PBS) and mounted in VECTASHIELD® mounting medium for fluorescence (Vector Laboratories, Inc., Burlingame, CA, US) or DAKO fluorescent mounting medium. In some cases, antigen retrieval procedure (S1699, DAKO) was applied before the blocking step. Single plane images were acquired at 20x magnification and identical settings between mutant samples and controls were used. Stainings were documented by confocal microscopy (Zeiss LSM700 and LSM800) Optical sections were 2 μm in 20X overview pictures unless specified.

RNAscope® *in situ* hybridization

In situ hybridization assay (ISH, RNAscope®, Advanced Cell Diagnostics, Inc., ACDBio, Newark, CA, US) was performed on embryo cryosections (fixed overnight in 4% PFA in PBS) at E10.5 (brachial (Br) and Lumbar (L)), E11.5, E12.5 and E18.5 on *Prdm12*$^{+/+}$ and *Prdm12*$^{LZ/LZ}$, *Ngn1*$^{+/+}$, *Ngn1*$^{-/-}$, *Ngn2*$^{+/+}$ and *Ngn2*$^{-/-}$. RNAscope® was performed using the manufacturer's instructions (ACDBio). The following probes have been used in this study: Mm-Prdm12 # 524371, Mm-Neurog1 #414211 and Mm-Neurog2 #417291. For fluorophore labeling, the AMP 4 Alt C-FL option was employed resulting in probe labeling with Atto 550 (Figures 1B and S1G) and the subsequent immunohistochemistry (IHC) protocol described above was performed with some minor alterations (all primary antibody concentrations were 1:100). Alternatively, we used for fluorophore labeling the TSA Cy3, Cy5 and Fluorescein evaluation kit (Perkin Elmer; Figures 3E and 3F). Images were acquired as described above.

Whole mount Immunofluorescence

Whole-mount immunofluorescent staining was previously described[14] and performed as followed. Following samples fixation (4% PFA for 4h at 4°C with rotation 72 rpm) and PBS washes (with rotation 72 rpm, 3 times 10min), autofluorescence from the blood was beached with incubation in Dent's bleach (one part 30% H_2O_2, two parts Dent's fix) (Dent's Fix: 20% DMSO, 80% MetOH) at 4°C for 24h. Next the samples were washed in MetOH at room temperature 5 times, 10min each and then fixed in Dent's Fix solution for 24h at 4°C.

On the day of the staining, the samples were rinsed in PBS three times and then washed in PBS at room temperature with rotation. Samples were then incubated with the primary antibodies (anti-Peripherin, anti-TrkA and anti-Neurofilament 160, see Key Resources Table for details) into blocking solution (5% normal donkey serum, 20% DMSO in PBS) for a week, at room temperature with rotation (72 rpm). The samples were rinsed in PBS and washed 6 times in washing buffer (0.1% Triton X-100, PBS) for 30min each and incubated in secondary antibodies in blocking solution for 2-3 days at room temperature with rotation. Finally, the samples were rinsed then washed six times in washing buffer at room temperature, 30min each and dehydrated in 50% MetOH/PBS and then, 3 times 20min in 100% MetOH. Prior to imaging, the samples were cleared in BABB solution (one part benzyl alcohol, two parts benzyl benzoate) and imaged in BABB. Z stacks images were collected and 2D projections were created using the Zeiss LSM image processing software.

In ovo electroporation

A control plasmid pCAGeGFP or our construct of interest pCAG-FLAG-mPRDM12-IRES-puro[15], were injected *in ovo* into the neural tube of HHst13/14 chick embryos (plasmids concentration 1μg/μl. Electroporation as described previously[16] and performed as

followed. Five pulses of 50V/cm was performed using a square wave electroporator (BTX). Embryos were collected at 96h post electroporation and processed for immunostaining. The transfection efficiency was high in both condition, eGFP and FLAG-PRDM12, as seen with the numerous eGFP^{+} and FLAG-labeled PRDM12^{+} cells in the electroporated side of the neural tube.

Electron microscopy

Sciatic nerves from E18.5 old *Prdm12*$^{-/-}$ and control mice were used. Nerves were fixed with 2.5% glutaraldehyde in 0.1 M sodium cacodylate buffer (pH 7.3; over-night at 4°C) and then treated with 1% OsO4 in sodium cacodylate buffer at 4°C for 4h. Samples were embedded in epoxy resin according to the manufacturer's (Sigma) protocol, cut and contrasted by lead citrate and uranyl acetate for ultra-thin analysis. Imaging was performed with the FEI Tecnai Spirit BioTWIN electron microscope (Thermo Fischer Scientific).

QUANTIFICATION AND STATISTICAL ANALYSIS

For cell type quantifications ImageJ software was used. Only progenitors, glial cells or neurons with a visible nucleus were considered for analysis. Quantification of molecular markers in the dorsal root ganglia was carried out on a minimum of 5 DRGs sections or more per animal, per condition (see figure legends for n's and genotypes).

Data were analyzed using GraphPad Prism 5 and expressed as mean ± s.e.m. The statistical test performed is reported in the figure legend. t tests were two-sided. Legend for significance: *$p \leq 0.05$, **$p \leq 0.01$, ***$p \leq 0.001$. Data distribution was assumed to be normal. No animals or data points were excluded from the analyses. No statistical methods were used to pre-determine sample size but our sample size are similar to those generally employed in the field.